[CANCER RESEARCH 64, 3276–3280, May 1, 2004]

Antitumor Activity of a Kinesin Inhibitor

Roman Sakowicz,[2] Jeffrey T. Finer,[2] Christophe Beraud,[2] Anne Crompton,[2] Evan Lewis,[2] Alex Fritsch,[2] Yan Lee,[2] John Mak,[2] Robert Moody,[2] Rebecca Turincio,[2] John C. Chabala,[2] Paul Gonzales,[1] Stephanie Roth,[1] Steve Weitman,[1] and Kenneth W. Wood[2]

[1]Institute for Drug Development, Cancer Therapy and Research Center, San Antonio, Texas; and [2]Cytokinetics, Inc., South San Francisco, California

ABSTRACT

Several members of the kinesin family of microtubule motor proteins play essential roles in mitotic spindle function and are potential targets for the discovery of novel antimitotic cancer therapies. KSP, also known as *Hs*Eg5, is a kinesin that plays an essential role in formation of a bipolar mitotic spindle and is required for cell cycle progression through mitosis. We identified a potent inhibitor of KSP, CK0106023, which causes mitotic arrest and growth inhibition in several human tumor cell lines. Here we show that CK0106023 is an allosteric inhibitor of KSP motor domain ATPase with a K_i of 12 nM. Among five kinesins tested, CK0106023 was specific for KSP. In tumor-bearing mice, CK0106023 exhibited antitumor activity comparable to or exceeding that of paclitaxel and caused the formation of monopolar mitotic figures identical to those produced in cultured cells. KSP was most abundant in proliferating human tissues and was absent from cultured postmitotic neurons. These findings are the first to demonstrate the feasibility of targeting mitotic kinesins for the treatment of cancer.

INTRODUCTION

Drugs that perturb mitosis have proven clinically effective in the treatment of many cancers (1). Despite the diverse array of essential spindle proteins that could be exploited as targets for the discovery of novel cancer therapies, all spindle-targeted therapeutics in clinical use today act on only one protein, tubulin.

Kinesin motor proteins play multiple roles in microtubule-dependent intracellular trafficking. All members of the kinesin superfamily share a catalytic "motor" domain of ~350–450 amino acids that is responsible for movement along the microtubule. This compact domain mediates interaction with microtubules and with ATP, and translates energy released by ATP hydrolysis into motile force (2). Regions outside the motor domains of kinesin family members are quite divergent and play important roles in translating force generated by the motor domain to specific intracellular cargos (3). Several kinesins play essential roles in mitotic spindle assembly and function (1).

In organisms ranging from fungi to humans, the mitotic kinesin KSP and closely related kinesins of the BimC subfamily (4) function at the earliest stages of mitosis to mediate centrosome separation and formation of a bipolar mitotic spindle (5–13). Failure of KSP function leads to cell cycle arrest in mitosis with a monopolar mitotic spindle (5, 6, 9). KSP expression is most abundant in proliferating human tissues, including thymus, tonsils, testis, esophageal epithelium, and bone marrow, and is absent from postmitotic human central nervous system neurons (see Supplementary Fig. 1), consistent with an exclusive role for KSP in cell proliferation. These data suggest that KSP would be an attractive target for the discovery of novel and specific antimitotic cancer therapies that should not disrupt microtubule-based cellular processes, such as neuronal transport, that are unrelated to proliferation.

We describe here the identification and characterization of CK0106023, a potent and specific allosteric inhibitor of KSP ATPase activity, and demonstrate that CK0106023 exhibits antitumor activity.

MATERIALS AND METHODS

Biochemistry. The motor domains of KSP (amino acids 1–360), HsMKLP-1 (amino acids 4–433), HsCENP-E (amino acids 2–340), and HsKif1A (amino acids 3–353) were all expressed as in *Escherichia coli* BL21(DE3) as COOH-terminal 6-his fusion proteins. Bacterial pellets were lysed in a microfluidizer (Microfluidics Corp.) with a lysis buffer [50 mM Tris-HCl; 50 mM KCl, 10 mM imidazole, 2 mM $MgCl_2$, 8 mM β-mercaptoethanol, 0.1 mM ATP (pH 7.4)], and proteins were purified using Ni-NTA agarose affinity chromatography, with an elution buffer consisting of 50 mM PIPES, 10% sucrose, 300 mM imidazole, 50 mM KCl, 2 mM $MgCl_2$, mM β-mercaptoethanol, and 0.1 mM ATP (pH 6.8).

Steady-state measurements of ATPase activity were performed with a pyruvate kinase–lactate dehydrogenase detection system that coupled the appearance of ADP with oxidation of NADH. Absorbance changes were monitored at 340 nm. All biochemical experiments were performed in PEM25 buffer [25 mM Pipes/KOH (pH 6.8), 2 mM $MgCl_2$, 1 mM EGTA] supplemented with 10 μM Taxol for experiments involving microtubules. Rates of ADP release were measured in a stopped-flow apparatus (Hi-Tech Scientific); the decrease in fluorescence of MANT-ATP (Molecular Probes) was monitored, as described previously (14). Rates of P_i release were measured in a stopped-flow apparatus, using bacterial phosphate binding protein modified with 7-diethylamino-3-((((2 maleimidyl)ethyl)amino)carbonyl)coumarin (MDCC) dye as described previously (15). K_i estimates of KSP inhibitors were extracted from the dose–response curves, with explicit correction for enzyme concentration (16).

We monitored tubulin polymerization by measuring changes in absorbance at 340 nm (17). The assay was performed in 100-μl volumes in 96-well half-area microtiter plates (Costar), using a microplate reader (Molecular Devices, Inc.) with the incubation temperature set at 37°C.

CK0106023 enantiomers were separated by chiral phase preparative HPLC on a Chiralpak-AD column [amylose tris-(3,5-dimethylphenylcarbamate) coated on a 10-μm silica gel substrate; 250 × 20 mm (length × inside diameter); Chiral Technologies, Inc., Exton, PA] with ethyl acetate–hexanes (7:3, v/v) as eluent.

Cell Biology. All cells were cultured in 10% FCS in RPMI 1640 in 5% CO_2. We assessed 48-h growth inhibition by serial dilution of CK0106023 relative to DMSO-treated cells in 96-well microtiter plates, using 3-(4, 5-dimethylthiazol-2-yl)-5-(3-carboxymethoxyphenyl)-2-(4-sulfophenyl)-2*H*-tetrazolium (Promega Corp., Madison, WI) according to the manufacturer's instructions. Cell growth was represented as the ratio of absorbance of treated cells to DMSO control, plotted by concentration and fitted to a four-parameter curve. Concentrations at which cellular growth was inhibited by 50% were extrapolated from the curve fit.

The DNA content of HeLa cells cultured in the presence or absence of 1 μM CK0106023 for 24 h was assessed by propidium iodide staining and flow cytometry (FACSCaliber; BD Biosciences Immunocytometry Systems).

Immunofluorescence images were collected of HeLa cells treated for 24 h with 1 μM CK0106023, fixed with 2% formaldehyde, permeabilized, and stained with DM1-α (Sigma), anti-γ-tubulin (Sigma), and 1 μg/ml 4′,6-diamidino-2-phenylindole (Sigma); and with Alexa 488 secondary goat anti-rabbit IgG (Molecular Probes) and Rhodamine-X goat antimouse IgG (Jackson ImmunoResearch Laboratories, Inc.). Images were collected with a DeltaVi-

Received 12/8/03; revised 2/29/04; accepted 2/25/04.

Grant support: Cytokinetics, Inc.

The costs of publication of this article were defrayed in part by the payment of page charges. This article must therefore be hereby marked *advertisement* in accordance with 18 U.S.C. Section 1734 solely to indicate this fact.

Note: Supplementary data for this article can be found at Cancer Research Online (http://cancerres.aacrjournals.org).

Requests for reprints: Kenneth W. Wood, Cytokinetics, Inc., 280 East Grand Avenue, South San Francisco, CA 94080. E-mail: kwood@cytokinetics.com.

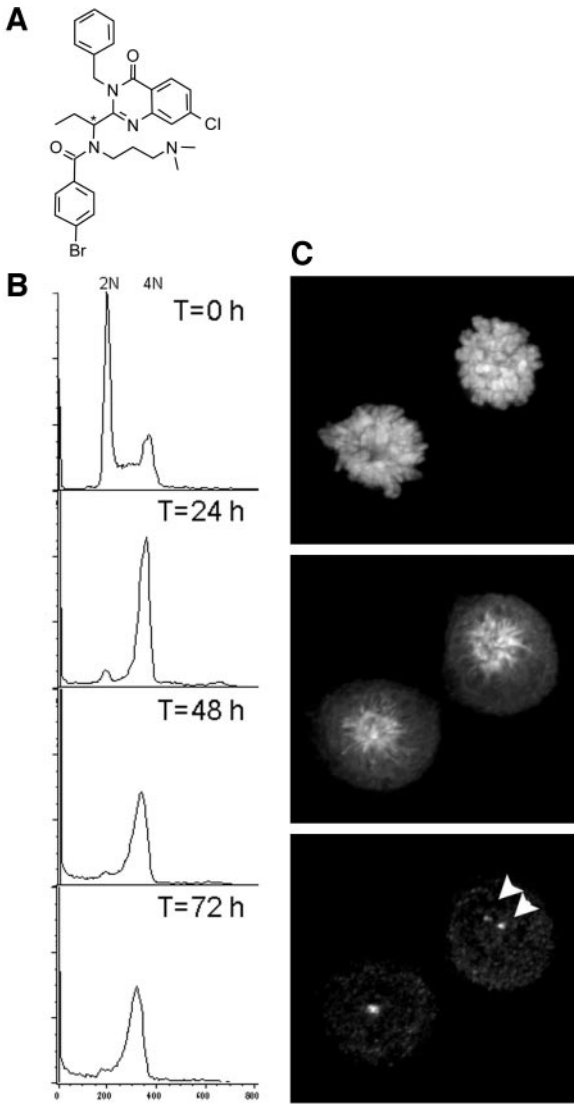

Fig. 1. Structure and activity of CK0106023. *A*, CK0106023 structure, with single chiral center indicated by *; K_i (KSP) = 12 nM. *B*, cell cycle distribution of HeLa cells treated with 1 μM CK0106023 for the indicated times. *C*, immunofluorescence images of HeLa cells treated with 1 μM CK0106023 for 24 h and stained for DNA (*top panel*) α-tubulin (*middle panel*), and γ-tubulin, a centrosomal marker (*bottom panel*). *Arrows* indicate unseparated centrosomes.

sion Restoration Microscopy System (Applied Precision) at a magnification of $\times$600. Z stacks (0.2 μm) were collected, and out of focus information was removed by constrained iterative deconvolution. Z stacks were then compressed into to a single image plane.

Tumor Studies. All drugs were formulated in 10% ethanol–10% cremaphor in water and administered by i.p. injection. Antitumor efficacy was assessed in female nude mice that had received s.c. trochar implants containing fragments of human SKOV3 tumors harvested from nude mice hosts. Animals were pair-matched into treatment and control groups of eight mice each and daily 5$\times$ dosing was begun with vehicle, 20 mg/kg paclitaxel, or CK0106023 at 25 and 50 mg/kg. Mice were weighed twice weekly, and tumor measurements were taken. The results were converted to tumor mass (mg) by the formula: Width^2 $\times$ Length/2. All mice were sacrificed when mean tumor mass in the vehicle control group reached 1 g. Tumors were excised and weighed, and the percentage of tumor growth inhibition was calculated relative to the vehicle control group. Statistical significance was calculated by use of a two-sample *t* test. Tumors shrinking to masses less than the mass recorded on day 1 were scored as partial regressions.

Sections of formalin-fixed tumors were prepared from mice sacrificed 1 day after the last of four daily 50 mg/kg doses of CK0106023 or vehicle. Sections were stained with H&E and visualized by bright-field microscopy.

Expression Profiling. Tissues were obtained from the Cooperative Human Tissue Network (Philadelphia, PA) and National Disease Research Interchange (Philadelphia, PA). NT-2 cells and differentiated NT2-N neurons were obtained from Layton BioScience (Atherton, CA) and prepared as described by Pleasure and Lee (18). Total RNA was extracted with a ToTALLY RNA kit (Ambion; Austin, TX) according to the manufacturer's protocol. DNase-treated total RNA was reverse-transcribed with random hexamers, and real-time quantitative PCR TaqMan assays were performed with KSP- or β-glucuronidase-specific primers on the GeneAmp 5700 Sequence Detection System (Applied Biosystems, Foster City, CA), using the manufacturer's standard curve method. KSP mRNA levels were expressed relative to endogenous levels of β-glucuronidase mRNA and normalized to the KSP:β-glucuronidase expression level in proliferating HeLa cells (HeLa = 1000). Extracts of NT2 and postmitotic NT2-N cells (18) were immunoblotted using antibodies directed against KSP/Eg5 (19), against α-tubulin (DM1-α), and against proliferating cell nuclear antigen (PC10; Sigma-Aldrich, Inc.). SE were calculated for each group of samples measured.

RESULTS AND DISCUSSION

The defining structural feature of kinesins is the motor domain. This relatively compact domain is responsible for ATP hydrolysis and generation of motile force along the microtubule (2, 20). We screened a collection of small synthetic organic compounds for inhibitors of KSP motor domain activity and identified a series of quinazolinone inhibitors of KSP (21). Synthetic chemical optimization improved the biochemical potency of these compounds >100-fold, leading to identification of CK0106023 (Fig. 1*A*), which inhibits KSP ATPase activity with a K_i of 12 nM.

CK0106023 is a potent inhibitor of cell cycle progression. Exposure of cultured cells to CK0106023 produces an accumulation of cells with 4N DNA content peaking at 24 h and persisting for at least 72 h, consistent with arrest in mitosis (Fig. 1*B*). Examination by immunofluorescence microscopy confirmed arrest in M-phase (Fig. 1*C*). CK0106023 produced a rosette of condensed mitotic chromosomes attached to a radial array of microtubules indistinguishable from that observed after microinjection of antibody directed against KSP (6) or after treatment with monastrol (9, 22). Staining with antibody directed against γ-tubulin, a centrosomal marker, revealed the presence of two centrosomes at the center of these figures (Fig. 1*C*, *bottom panel*), indicating a failure of centrosome separation and consequent formation of a monopolar mitotic spindle. This mitotic arrest results in potent inhibition of the growth in a variety of human tumor cell lines (Table 1). The mean growth inhibitory activity of CK0106023 toward these human cell lines was 364 nM, with activity against each line, including the three multidrug-resistant lines NCI/ADR-RES, HCT-15, and A2780ADR (Table 1), varying less than 5-fold.

Interaction of CK0106023 with the KSP motor domain is very

Table 1 *CK0106023 cell growth inhibition*

Titration of cell growth *in vitro* by CK0106023 over 48 h. Each value represents the mean (SD) of at least two independent measurements (median number of measurements = 5).

Cell line	GI_{50}[a] (nM)	Cell/tumor type
SKOV3	126 ± 26	Ovarian carcinoma
A2780	191 ± 47	Ovarian carcinoma
A549	238 ± 77	Non-small cell lung carcinoma
NCI H460	307 ± 31	Non-small cell lung carcinoma
SF-268	297 ± 51	CNS
HT29	533 ± 135	Colon carcinoma
U2OS	426 ± 69	Osteosarcoma
DU145	466 ± 71	Prostate
A2780ADR	517 ± 127	Multidrug-resistant A2780
NCI/ADR-RES	582 ± 73	Multidrug-resistant
HCT-15	295 ± 68	Multidrug-resistant colon carcinoma
B16	399 ± 72	Murine melanoma

[a] GI_{50}, 50% growth inhibition; CNS, central nervous system.

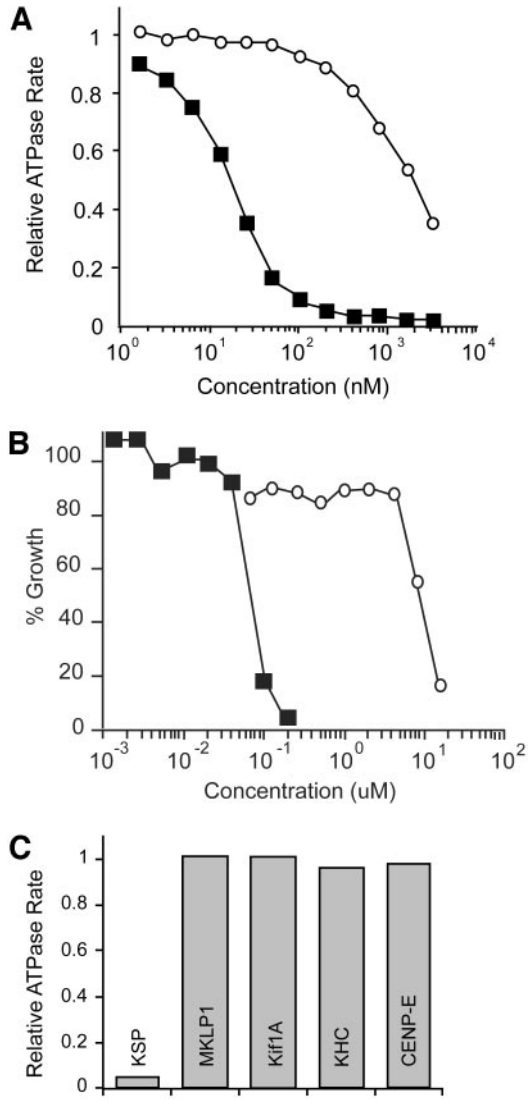

Fig. 2. CK0106023 specificity. *A*, titration of KSP ATPase activity with (*S*)-CK0106023 (○) and (*R*)-CK0106023 (■). *B*, growth inhibition of human SKOV3 ovarian carcinoma cells with (*S*)-CK0106023 (○) and (*R*)-CK0106023 (■). *C*, microtubule-stimulated ATPase rates of human kinesins in the presence of (*R*)-CK0106023 (3.4 μM) normalized to rates observed in the absence of the inhibitor. CK0106023 does not alter the kinetics of tubulin polymerization *in vitro* (see Supplementary Fig. 2). *KHC*, kinesin heavy chain.

specific. CK0106023 contains a single chiral center (Fig. 1*A*) and was initially identified as a racemic mixture of (*R*) and (*S*) enantiomers. These two enantiomers differ >1000-fold in their ability to inhibit KSP ATPase activity, with the vast majority of activity attributable to (*R*)-CK0106023 (Fig. 2*A*). Stereospecificity was also apparent in the cellular activity of CK0106023 (Fig. 2*B*). (*S*)-CK0106023 was at least 100-fold less effective at inhibiting cell growth than (*R*)-CK0106023. Lastly, among five kinesins tested, the activity of (*R*)-CK0106023 was specific for KSP (Fig. 2*C*). At 3.4 μM, more than 200-fold the K_i toward KSP, no inhibitory activity was apparent toward the mitotic kinesins CENP-E and MKLP1, toward the ubiquitous kinesin heavy chain, or toward the neuronal kinesin Kif1A. CK0106023 also had no effect on the kinetics of microtubule polymerization *in vitro* (see Supplementary Fig. 2). These data strongly indicate that the antimitotic, growth-inhibitory activity of CK0106023 is attributable exclusively to inhibition of KSP motor activity.

The kinesin motor domain undergoes a complex kinetic cycle of ATP binding, nucleotide hydrolysis, and sequential release of the products P_i and ADP, respectively (23). This cycle is tightly coupled to force generation and movement by conformational changes of the motor domain (24). Interaction of the kinesin motor domain with microtubules accelerates the rate of nucleotide hydrolysis by increasing the rate of the limiting step of ADP release by 100-1000-fold (25, 26). The microtubule-stimulated ATPase activity of kinesins is thus a sensitive readout of mechanical and catalytic competency of the enzyme. Inhibition of microtubule-stimulated ATPase could result from competitive displacement of ATP, interference with microtubule binding, or allosteric disruption of the functional linkage between nucleotide and microtubule binding sites. Inhibitors representing each of these three mechanisms have been reported (5, 22, 27, 28). One of these, monastrol, is an allosteric inhibitor specific for KSP/Eg5 (5, 22).

We found that CK0106023 inhibition of KSP motor domain ATPase was due to dramatic slowing of the rate of ADP release (Fig. 3). Rates of ADP release were monitored under transient conditions

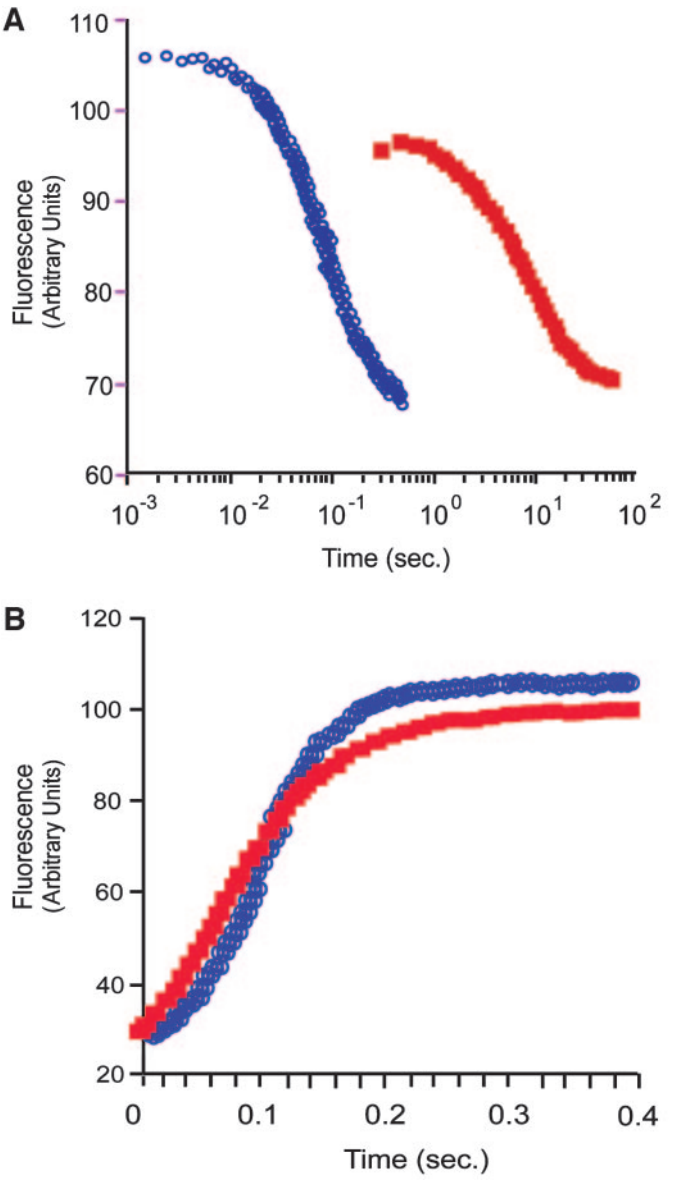

Fig. 3. Mechanism of KSP inhibition by CK0106023. *A*, slowing of microtubule-stimulated ADP release by (*R*)-CK0106023 (*red*) compared with DMSO (*blue*) as detected by decrease in MANT-ADP fluorescence (note log time scale). *B*, release of P_i in the presence of DMSO (*blue*) or 3.4 μM (*R*)-CK0106023 (*red*), detected by increased fluorescence of MDCC-modified bacterial phosphate binding protein (15).

Table 2 *Effects of CK0106023 on rates of ADP release*

Rates of ADP release (s^{-1}) in the presence and absence of microtubules in the presence and absence of 3.4 μM (*R*)-CK0106023.

	DMSO	(*R*)-CK0106023
(+) MT[a]	$28.50s^{-1}$	$0.470s^{-1}$
(−) MT	$0.12s^{-1}$	$0.006s^{-1}$

[a] MT, microtubules.

Table 3 *Tumor response and toxicity*

Average percentage of tumor growth inhibition, number of partial regressions at study end (day 15), average weight loss on day 8 compared with day 1, and mortality.

		CK0106023		Paclitaxel
	Vehicle	25 mg/kg	50 mg/kg	(20 mg/kg)
% TGI[a]	NA	71	NA	73
Partial regressions (*n*)	0	1	6	0
Weight change (%)	2.7	3.2	−11.16	−8.5
Mortalities (*n*)	0	0	2	0

[a] % TGI, tumor growth inhibition; NA, not applicable.

by use of MANT-ADP, a fluorescent ADP analog that exhibits enhanced fluorescence when bound to enzyme and less fluorescence when free in solution (14). The changes in MANT-ADP fluorescence observed over time after rapid mixing with microtubules in the presence and absence of (*R*)-CK0106023 are displayed on a log scale in Fig. 3*A* to accommodate the dramatically different observed rates of release. The decreased rate of ADP release induced by (*R*)-CK0106023 is reflected by the rightward shift of the curve depicting changes in MANT-ADP fluorescence over time compared with control (Fig. 3*A*). This shift corresponds to a 60-fold reduction in the rate of ADP release observed in the presence of microtubules (Table 2). Interestingly, CK0106023 also inhibited the basal rate of ADP release to a similar degree, indicating that the effect is not dependent on the presence of microtubules (Table 2). We observed no effect on the rate of P_i release (Fig. 3*B*). These findings are consistent with observations made under steady-state conditions demonstrating that CK0106023 is uncompetitive with ATP and noncompetitive with microtubules (see Supplementary Fig. 3). Together, these data indicate that CK0106023 is an allosteric inhibitor of KSP motor domain function that specifically slows ADP release and does not directly disrupt KSP motor domain binding to microtubules or inhibit binding to or hydrolysis of ATP.

The strong antimitotic activity displayed by CK0106023 against cultured cells prompted us to test CK0106023 for antitumor activity *in vivo*. On the basis of tests of a range of doses of CK0106023 in healthy, nontumor-bearing nude mice on a daily 5× schedule, we estimated that the maximum tolerated dose of CK0106023 was ~50 mg/kg. Doses of 50 and 25 mg/kg were administered daily for 5 days to nude mice bearing xenografts of the human ovarian carcinoma SKOV3. Paclitaxel at its maximum tolerated dose (20 mg/kg) served as a positive control.

CK0106023 administered at 25 mg/kg resulted in 71% tumor growth inhibition (Table 3, Fig. 4*A*), comparable to that produced by paclitaxel at its maximum tolerated dose (73% tumor growth inhibition; Fig. 4). The difference between the mean final tumor weights in animals receiving CK0106023 and those receiving vehicle control was statistically significant ($P < 0.05$). No statistical difference was detected between mean final tumor weights in animals receiving paclitaxel or 25 mg/kg CK0106023. One animal receiving 25 mg/kg experienced a partial tumor regression, with 56% tumor shrinkage relative to the tumor weight at the start of dosing. At 25 mg/kg, CK0106023 did not induce changes in body weight significantly different from the control group, whereas animals receiving paclitaxel experienced a nadir of nearly 9% weight loss on day 8, significantly more severe than observed in either the control or 25 mg/kg CK0106023 groups ($P < 0.04$). A dose of 50 mg/kg resulted in the death of two animals on day 8 and thus was above the maximum tolerated dose. However, partial tumor regressions were observed in all six surviving animals, producing mean tumor shrinkage of 55%. Mean body weight loss of these six animals was 11% on day 8. Recovery of body weight in all surviving animals suggested that the toxicities induced by both CK0106023 and paclitaxel are reversible.

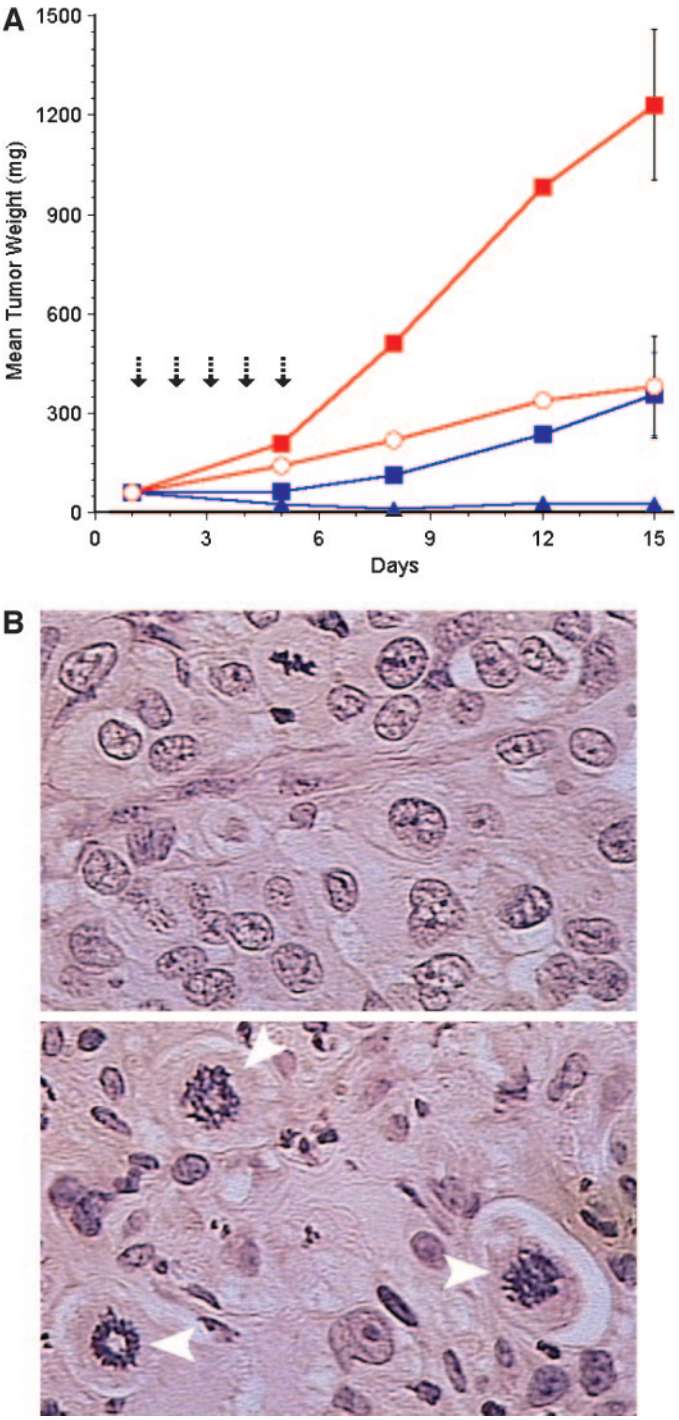

Fig. 4. Antitumor activity of CK0106023. *A*, plot of average tumor weights (log scale) from mice receiving vehicle (*red closed squares*), 20 mg/kg paclitaxel (*red open circles*), and CK0106023 at 25 (*blue closed squares*) and 50 mg/kg (*blue closed triangles*) administered 5 times daily (*arrows*). SE (*bars*) is displayed for final measured tumor weight. *B*, mitotic figures in histological sections of tumors from mice receiving four daily doses of 50 mg/kg CK0106023 (boxed figures are indicated by *arrowheads* in the *bottom panel*) and from control animals (*top panel*).

The monopolar mitotic figures observed in cultured cells after exposure to CK0106023 were very distinctive at the light microscope level (Fig. 1*C*). To verify that the antitumor activity of CK0106023 was indeed the consequence of KSP inhibition, nude mice bearing SKOV3 tumors received daily doses of 50 mg/kg CK0106023 for a total of 4 days. On day 5, animals were sacrificed, the tumors were removed and fixed, and paraffin sections were prepared and stained. Circular mitotic figures, similar to the monopolar spindles seen in CK0106023-treated cells in culture, were clearly visible in tumors from animals treated with CK0106023 but not in vehicle-treated controls (Fig. 4*B*).

CK0106023 is the first agent targeting a mitotic kinesin with demonstrated antitumor activity. The profile of KSP mRNA expression in normal human tissues and the absence of KSP protein from postmitotic neurons are consistent with an exclusive role for KSP in cell proliferation. These data, together with the biochemical specificity of CK0106023, suggest that specific inhibitors of KSP may have clinical utility in the treatment of cancer.

ACKNOWLEDGMENTS

We thank James Sabry, Ron Vale, Larry Goldstein, and Jim Spudich for advice and encouragement; Fady Malik, Eugeni Vaisberg, Cindy Adams, and other Cytokinetics team members for discussions and critical advice; Ming Yu and Jessie Jia for expert technical assistance; Gregory Alexander and Daniel Coleman for advice on statistical analysis; Robert Blum and Sheila Vaughan for their support; Duane Compton and Rebecca Heald for providing antibodies; and Lisa Belmont for collecting immunofluorescence images.

REFERENCES

1. Wood KW, Cornwell WD, Jackson JR. Past and future of the mitotic spindle as an oncology target. Curr Opin Pharmacol 2001;1:370–7.
2. Vale RD, Milligan RA. The way things move: looking under the hood of molecular motor proteins. Science (Wash DC) 2000;288:88–95.
3. Goldstein LS, Philp AV. The road less traveled: emerging principles of kinesin motor utilization. Annu Rev Cell Dev Biol 1999;15:141–83.
4. Kim AJ, Endow SA. A kinesin family tree. J Cell Sci 2000;113(Pt 21):3681–2.
5. Mayer TU, Kapoor TM, Haggarty SJ, King RW, Schreiber SL, Mitchison TJ. Small molecule inhibitor of mitotic spindle bipolarity identified in a phenotype-based screen. Science (Wash DC) 1999;286:971–4.
6. Blangy A, Lane HA, d'Herin P, Harper M, Kress M, Nigg EA. Phosphorylation by p34cdc2 regulates spindle association of human Eg5, a kinesin-related motor essential for bipolar spindle formation in vivo. Cell 1995;83:1159–69.
7. Heck MM, Pereira A, Pesavento P, Yannoni Y, Spradling AC, Goldstein LS. The kinesin-like protein KLP61F is essential for mitosis in Drosophila. J Cell Biol 1993;123:665–79.
8. Hoyt MA, He L, Loo KK, Saunders WS. Two Saccharomyces cerevisiae kinesin-related gene products required for mitotic spindle assembly. J Cell Biol 1992;118:109–20.
9. Kapoor TM, Mayer TU, Coughlin ML, Mitchison TJ. Probing spindle assembly mechanisms with monastrol, a small molecule inhibitor of the mitotic kinesin, Eg5. J Cell Biol 2000;150:975–88.
10. Roof DM, Meluh PB, Rose MD. Kinesin-related proteins required for assembly of the mitotic spindle. J Cell Biol 1992;118:95–108.
11. Sawin KE, LeGuellec K, Philippe M, Mitchison TJ. Mitotic spindle organization by a plus-end-directed microtubule motor. Nature (Lond) 1992;359:540–3.
12. Hagan I, Yanagida M. Novel potential mitotic motor protein encoded by the fission yeast cut7+ gene. Nature (Lond) 1990;347:563–6.
13. Enos AP, Morris NR. Mutation of a gene that encodes a kinesin- like protein blocks nuclear division in A. nidulans. Cell 1990;60:1019–27.
14. Gilbert SP, Mackey AT. Kinetics: a tool to study molecular motors. Methods 2000;22:337–54.
15. Brune M, Hunter JL, Corrie JE, Webb MR. Direct, real-time measurement of rapid inorganic phosphate release using a novel fluorescent probe and its application to actomyosin subfragment 1 ATPase. Biochemistry 1994;33:8262–71.
16. Blanchoin L, Pollard TD. Mechanism of interaction of Acanthamoeba actophorin (ADF/Cofilin) with actin filaments. J Biol Chem 1999;274:15538–46.
17. Carlier MF, Pantaloni D. Kinetic analysis of cooperativity in tubulin polymerization in the presence of guanosine di- or triphosphate nucleotides. Biochemistry 1978;17:1908–15.
18. Pleasure SJ, Lee VM. NTera 2 cells: a human cell line which displays characteristics expected of a human committed neuronal progenitor cell. J Neurosci Res 1993;35:585–602.
19. Mountain V, Simerly C, Howard L, Ando A, Schatten G, Compton DA. The kinesin-related protein, HSET, opposes the activity of Eg5 and cross-links microtubules in the mammalian mitotic spindle. J Cell Biol 1999;147:351–66.
20. Yang JT, Saxton WM, Stewart RJ, Raff EC, Goldstein LS. Evidence that the head of kinesin is sufficient for force generation and motility in vitro. Science (Wash DC) 1990;249:42–7.
21. Finer JT, Bergnes G, Feng B, Smith WW, Chabala JC. Methods and compositions utilizing quinazolinones. PCT Int. Appl. WO 01/030768: Cytokinetics, Inc., 2001.
22. Maliga Z, Kapoor T, Mitchison T. Evidence that monastrol is an allosteric inhibitor of the mitotic kinesin Eg5. Chem Biol 2002;9:989.
23. Moyer ML, Gilbert SP, Johnson KA. Pathway of ATP hydrolysis by monomeric and dimeric kinesin. Biochemistry 1998;37:800–13.
24. Endow SA. Processive and nonprocessive models of kinesin movement. Annu Rev Physiol 2002;65:161–75.
25. Hackney DD. Kinesin ATPase: rate-limiting ADP release. Proc Natl Acad Sci USA 1988;85:6314–8.
26. Kuznetsov SA, Gelfand VI. Bovine brain kinesin is a microtubule-activated ATPase. Proc Natl Acad Sci USA 1986;83:8530–4.
27. Sakowicz R, Berdelis MS, Ray K, et al. A marine natural product inhibitor of kinesin motors. Science (Wash DC) 1998;280:292–5.
28. Shimizu T, Furusawa K, Ohashi S, et al. Nucleotide specificity of the enzymatic and motile activities of dynein, kinesin, and heavy meromyosin. J Cell Biol 1991;112:1189–97.

Antitumor Activity of a Kinesin Inhibitor

Roman Sakowicz, Jeffrey T. Finer, Christophe Beraud, et al.

Cancer Res 2004;64:3276-3280.